Ligand-binding properties and structural characterization of a novel rat odorant-binding protein variant

Loïc Briand, Claude Nespoulous, Valérie Perez, Jean-Jacques Rémy, Jean-Claude Huet, Jean-Claude Pernollet

Eur. J. Biochem. **267**, 3079–3089 (2000) © FEBS 2000

Ligand-binding properties and structural characterization of a novel rat odorant-binding protein variant

Loïc Briand[1], Claude Nespoulous[1], Valérie Perez[1], Jean-Jacques Rémy[2], Jean-Claude Huet[1] and Jean-Claude Pernollet[1]

[1]*Biochimie et Structure des Protéines, Unité de recherches INRA, Jouy-en-Josas, France;* [2]*Biologie Cellulaire et Moléculaire, Unité de recherches INRA, Jouy-en-Josas, France*

After characterization of a novel odorant-binding protein (OBP) variant isolated from the rat nasal mucus, the corresponding cDNA was cloned by RT-PCR. Recombinant OBP-1F, the sequence of which is close to that of previously reported rat OBP-1, has been secreted by the yeast *Pichia pastoris* at a concentration of 80 $mg \cdot L^{-1}$ in a form identical to the natural protein as shown by MS, N-terminal sequencing and CD. We observed that, in contrast with porcine OBP-1, purified recombinant OBP-1F is a homodimer exhibiting two disulfide bonds (C44–C48 and C63–C155), a pairing close to that of hamster aphrodisin. OBP-1F interacts with fluorescent probe 1-aminoanthracene (1-AMA) with a dissociation constant of 0.6 ± 0.3 μM. Fluorescence experiments revealed that 1-AMA was displaced efficiently by molecules including usual solvents such as EtOH and dimethylsulfoxide. Owing to the large OBP-1F amounts expressed, we set up a novel biomimetic assay (volatile-odorant binding assay) to study the uptake of airborne odorants without radiolabelling and attempted to understand the odorant capture by OBP in the nasal mucus under natural conditions. The assay permitted observations on the binding of airborne odorants of different chemical structures and odors (2-isobutyl-3-methoxypyrazine, linalool, isoamyl acetate, 1-octanal, 1-octanol, dimethyl disulfide and methyl thiobutyrate). Uptake of airborne odorants in nearly physiological conditions strengthens the role of OBP as volatile hydrophobic odorant carriers in the mucus of the olfactory epithelium through the aqueous barrier towards the chemo-sensory cells.

Keywords: heterologous expression; odorant-binding protein; olfaction; *Pichia pastoris*; rat.

In order to reach their membrane receptors embedded in the membrane of the olfactory neurons, airborne odorants, which are commonly hydrophobic molecules, have to be conveyed through the aqueous nasal mucus by carriers. The odorant-binding proteins (OBP), which are abundant low-molecular mass soluble proteins (≈ 20 kDa) secreted by the olfactory epithelium in the nasal mucus of vertebrates, have been thought to play such a role [1]. These proteins reversibly bind odorants with dissociation constants in the micromolar range. Although their functions are still unclear, OBP are also suspected to participate in the deactivation of odorants [2]. Most OBP are homodimers, but monomers and heterodimers have also been reported [3–6]. X-ray analysis has revealed that bovine and porcine OBP are folded in the typical β-barrel structure of lipocalins [7–9]. OBP have been identified in a variety of species, including pig, rabbit, mouse and rat [5,6,10–12] since the discovery of the first vertebrate OBP isolated from the bovine nasal mucus [3,13]. Different OBP subtypes have been reported to occur simultaneously in the same animal species, two in pig [5,14], four in mouse [15–17], three in rabbit [4] and at least eight in porcupine [18]. In rat, two OBP (called OBP-1 and OBP-2) have been cloned with quite different sequences [12,19,20]. The latter was specifically found in the vomeronasal organ and not in the olfactory epithelium [21]. Recently, their binding properties have been investigated demonstrating that the two rat OBP have distinct ligand specificity [22]. Whereas OBP-1 preferentially binds heterocyclic compouds, such as pyrazines, OBP-2 seems to be more specific for long-chain aliphatic aldehydes and carboxylic acids, providing the first evidence that different OBP subtypes are specially tuned towards a distinct class of odorants. The presence of four OBP subtypes in mouse suggests that more than two OBP could be isolated from the rat mucus.

Here we report the purification and the cloning of a novel rat OBP-1 variant called OBP-1F. Whereas to date binding studies have been restricted to the use of radiolabeled compounds or specific fluorescent probes for competitive binding experiments, we set up a general method (volatile-odorant binding assay, VOBA) for airborne odorant binding studies under physiological conditions without specific labeling. To obtain large quantities of rat OBP-1F necessary for the binding assay, we expressed the functional recombinant protein using the methylotrophic yeast *Pichia pastoris*. The secreted recombinant OBP-1F was purified and characterized precisely by MS, sequence analysis and CD. Its binding properties were studied using VOBA and 1-aminoanthracene (1-AMA) fluorescence to determine the number of binding sites and to compare the affinity of several odorants.

Correspondence to J.-C. Pernollet, Biochimie et Structure des Protéines, Unité INRA UR 477, Domaine de Vilvert, F-78352, Jouy-en-Josas Cedex, France. Fax: +33 1 34 65 27 65, Tel.: +33 1 34 65 27 50, E-mail: pernolle@jouy.inra.fr

Abbreviations: 1-AMA, 1-aminoanthracene; *AOX1*, gene encoding AOXI alcohol oxidase; IBMP, 2-isobutyl-3-methoxypyrazine; LC, liquid chromatography; OBP, odorant-binding protein; VOBA, volatile-odorant binding assay.

Enzyme: endoproteinase Glu-C (EC.3.4.21.19).

(Received 29 November 1999, revised 23 March 2000, accepted 24 March 2000)

MATERIALS AND METHODS

Strains and materials

Escherichia coli strain DH5α was used for DNA subcloning and propagation of the recombinant plasmid. *P. pastoris* strain GS115 (*his*4) was used in the expression study. Oligonucleotides were synthesized by Eurobio (France). PGEM-T vector was from Promega and pPIC9 and pPIC3.5K were from Invitrogen. Sinapinic acid and peptides for MALDI-TOF calibration were from Hewlett Packard. 1-AMA and all other chemicals were from Sigma. N-Terminal sequences were determined with reagents provided by PE Biosystems.

Protein purification

Eight-week-old Fischer rats (*Rattus norvegicus*) were killed under deep anesthesia. The nasal mucosa were removed and washed in NaCl/P_i, 180 mM NaCl, pH 7.3. The tissue samples were stored in liquid N_2 until required. The washing solution was centrifuged at 10 000 ***g*** for 20 min at 4 °C and used as the source of olfactory epithelium soluble proteins. Soluble proteins were submitted to anion-exchange chromatography using a Vydac QAE column (300 VHP, 0.75 i.d. × 5 cm, Interchim, France) pre-equilibrated with 20 mM Tris/HCl pH 8.0. After unbound protein washing, elution was achieved with the same buffer using a linear gradient from 0 to 0.5 M NaCl in 50 min. The flow rate was 0.5 mL·min^{-1} and the absorbance was recorded at 215 nm. The OBP-containing fractions were identified by MALDI-TOF with a HP G2025A Hewlett Packard equipment, using sinapinic acid as matrix. The OBP-containing fractions were pooled and submitted to reversed-phase HPLC on an Aquapore (C8) RP 300 column (0.21 i.d. × 3 cm, Brownlee, PerkinElmer, France) equilibrated with eluent A (0.1% trifluoroacetic acid in H_2O) and eluted with a linear gradient from 0 to 27% CH_3CN in 5 min, then up to 100% solvent B (60% CH_3CN, 40% H_2O, 0.09% trifluoroacetic acid) in 60 min. The flow rate was 0.2 mL·min^{-1} and the absorbance was recorded at 215 nm. The OBP-containing fractions were identified by liquid chromatography (LC) MS and N-terminal sequencing as described previously [23].

cDNA clone isolation and construction of the expression vector

Total RNA was isolated using RNAXEL extraction kit provided by Eurobio according to the manufacturer's recommendations. cDNA was prepared from the isolated total RNA by reverse transcription using reverse transcriptase from Gibco BRL Life Technologies. The cDNA encoding the native precursor OBP-1F was amplified by PCR using the following primers: RAT15′BglII, 5′-GAGCTCAGATCTAAACGATGGTGAAGTTTCTGCTGATT-3′ and OBP1Cterm, 5′-TGAAGCCATATGGAGTCT-3′. The first primer was designed after a sequence corresponding to the known rat OBP-1 presequence and the second to the noncoding OBP-1 nucleotide 3′ sequence [12]. The PCR-amplified fragment was cloned into the pGEM-T vector and six clones were sequenced. For the first construct, we used the primers 5′OBP1Fα, 5′-GTCTGCTACTCGAGAAAAGAGAGGCTGAAGCTGCACATCATGAAAATCTTGAT-3′ and RAT13′EcoRI 5′-CATATGGAATTCTTATTGGTTACAAGTGTC-3′ in order to amplify the mature OBP-1F. The PCR-amplified fragment was cloned into the *Xho*I and *Eco*RI sites of pPIC9, generating the plasmid pAlfOBP with the preprosequence of the α mating factor using the two Glu–Ala repeats between the α mating factor secretion peptide and the mature OBP-1F sequence. The cDNA encoding the native precursor OBP-1F was amplified by PCR using RAT15′BglII and RAT13′EcoRI. The PCR-amplified fragment was cloned into the *Bam*HI and *Eco*RI sites of pPIC3.5K generating the second construct pNatOBP. The constructs were confirmed by DNA sequencing using an ABI PRISM 310 sequencer (PE Biosystems, France).

Transformation of *P. pastoris* and screening for OBP expression

For transformation, the expression plasmid was linearized with *Bgl*II and later transferred into the *P. pastoris* yeast host by electroporation as described in the manual (version 3.0) of the *Pichia* expression Kit (Invitrogen). The selection of secreting clones, the culture production and the protein purification were achieved as described previously [23]. Briefly, having identified the best protein-producing His^+ Mut^S transformants by SDS/PAGE, and having determined the optimal expression time, shake-flask scale culture was carried out using an incubator Aerotron (Infors, France). Several colonies of a single isolate were used to inoculate 50 mL of buffered minimal glycerol-complex medium in a 500-mL baffled flask, which was then incubated at 29 °C, 300 r.p.m., continued for 16 h. Twenty mL of this preculture were then used to inoculate 1 L of buffered glycerol-complex medium divided between four 3-L baffled flasks. Incubation at 29 °C, 300 r.p.m. was continued for 2 days. At the end of this first phase of fermentation, the cell density reached about 100 g (wet weight) of cells per litre of culture. The cells were pelleted at 3000 ***g*** for 20 min at room temperature and the supernatant was discarded. The cells were resuspended in a total of 1 L of buffered minimal methanol medium at pH 6.0 in four sterile 3-L baffled flasks and incubation at 29 °C, 300 r.p.m. was continued for 4 days. During the induction period, MeOH was fed every 24 h in order to maintain a concentration of 0.5% (v/v).

Purification of the recombinant OBP

The supernatant was chilled and clarified by centrifugation at 10 000 ***g*** for 30 min at 4 °C. After filtration of the OBP-1F containing supernatant, it was equilibrated with 20 mM Tris/HCl pH 8.0 by dialysis for 4 days at 4 °C using a dialysis tube with 8000 Da cut-off (Servapor; Polylabo, France). OBP-1F was purified by anion-exchange chromatography using a Vydac QAE column (300 VHP, 0.75 i.d. × 5 cm; Interchim, France). After loading the dialyzed supernatant, the column was washed with 20 mM Tris/HCl pH 8.0 and the elution was achieved using a linear gradient with the same buffer from 0 to 0.5 M NaCl in 50 min. The flow rate was 0.5 mL·min^{-1} and the absorbance was recorded at 215 nm. The fractions containing OBP-1F were identified by MALDI-TOF, pooled and chromatographed by gel filtration. Exclusion-diffusion chromatography was performed through a 24-mL bed volume (1.0 i.d. × 30 cm) Pharmacia Superose 12 column. The gel was equilibrated with 50 mM ammonium acetate, pH 7.0, and elution carried out at 0.5 mL·min^{-1}. Finally the OBP-1F fractions were dialyzed extensively against MilliQ H_2O and lyophilized.

Recombinant OBP characterization

SDS/PAGE (16% acrylamide) was performed using a Mini-Protean II system (Bio-Rad, France) according to the method of Schägger and von Jagow [24] with modification [25]. The molecular mass calibration kits LMW and PMW (Pharmacia,

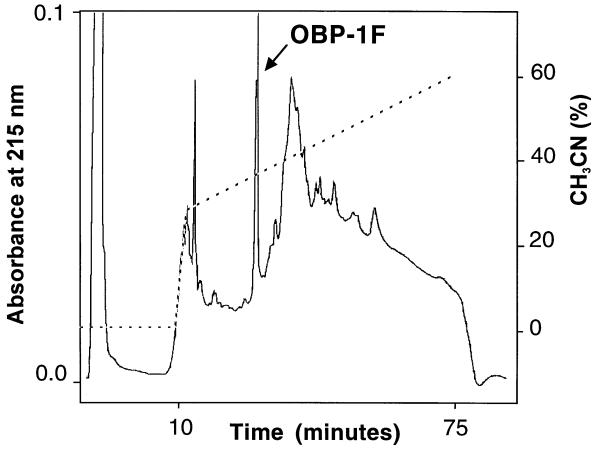

Fig. 1. Natural OBP purification from nasal mucus. Reversed-phase HPLC of the ion-exchange chromatography fraction containing OBP-1F on an Aquapore (C8) RP 300 column. Elution was performed with a bi-linear CH_3CN gradient (dashed line).

France) were used and the proteins stained with Serva blue G. Ion spray-MS was performed using an API 100 Sciex apparatus (PE Biosystems) linked to a 173 Microblotter (PE Biosystems). N-Terminal sequencing was conducted with a Procise PE Biosystems sequencer as described previously [23]. The oligomerization of the undenatured recombinant protein was studied by exclusion-diffusion chromatography on a 24-mL bed volume Superose 12 column (Pharmacia). The column was equilibrated in 100 mM potassium phosphate pH 7.5, 150 mM NaCl, at 0.5 $mL \cdot min^{-1}$. BSA (67 kDa), chicken egg ovalbumin (43 kDa), bovine β-lactoglobulin (36 kDa), carbonic anhydrase (30 kDa), soybean trypsin inhibitor (21.5 kDa) and bovine ribonuclease A (13.7 kDa) from Sigma, were used as standards. A 100-μL sample of purified OBP-1F was loaded at 1.0 $mg \cdot mL^{-1}$ onto the Superose column and the elution profiles were obtained from on-line UV detection at 280 nm. CD spectra were recorded using a Jobin-Yvon Mark V dichrograph and analyzed as described previously [26]. OBP-1F concentration was determined using UV spectroscopy using the extinction coefficient of 14 455 $M^{-1} \cdot cm^{-1}$ at 276 nm, calculated according to Pace *et al.* [27]. Protein samples (≈ 1 $mg \cdot mL^{-1}$ in 50 mM sodium phosphate buffer, pH 7.5) were placed in a 0.01-cm path length cell. Baseline was recorded with phosphate buffer. Structure proportions were computed with the algorithm of Deléage and Geourjon [28].

Disulfide bridge assignment

To determine the disulfide bridge pairing, unreduced OBP-1F was dissolved for 3 days in 1 M guanidinium chloride, then hydrolyzed with Glu-C endoproteinase Promega (enzyme/substrate ratio 1 : 20) in 50 mM sodium phosphate buffer, pH 7.8, in the presence of 0.3 M guanidinium chloride and 10% CH_3CN for 20 h at 25 °C. The digest was submitted to LC–MS analysis as described above. To quantify the extent of free thiols of the recombinant OBP-1F, the colorimetric reaction using 5,5′-dithiobis (2-nitrobenzoic acid) developed by Ellman [29] was performed. A 10-fold excess of Ellman's reagent over protein was used and the number of reactive cysteine residues was quantified by absorbance at 412 nm.

Fluorescence measurements using 1-AMA probe

Binding experiments were performed with either 2 or 10 μM OBP-1F solutions in 50 mM potassium phosphate buffer pH 7.5, using 1-AMA dissolved in 10% MeOH or in 95% EtOH as 1 mM stock solution. One μL successive aliquots were added to 1 mL of OBP-1F solution. Spectra were recorded at 25 °C using a SFM 25 Kontron fluorometer with a 5-nm bandwidth for both excitation and emission. No cut-off filter was used in the excitation beam. The relative proportion of ligand bound to OBP-1F was calculated by measuring fluorescence emission (expressed in arbitrary units) at 485 nm after excitation at 255 nm. Calculations were performed from a plot of fluorescence intensity vs. ligand concentration obtained with a nonlinear regression method [30] using DELTAGRAPH 4.5 software. The competitive binding assays contained 2 μM of OBP-1F and other proteins in 50 mM potassium phosphate buffer, pH 7.5. The competitor ligands MeOH, EtOH and dimethylsulfoxide were used pure and 2-isobutyl-3-methoxypyrazine (IBMP) was dissolved in 10% MeOH.

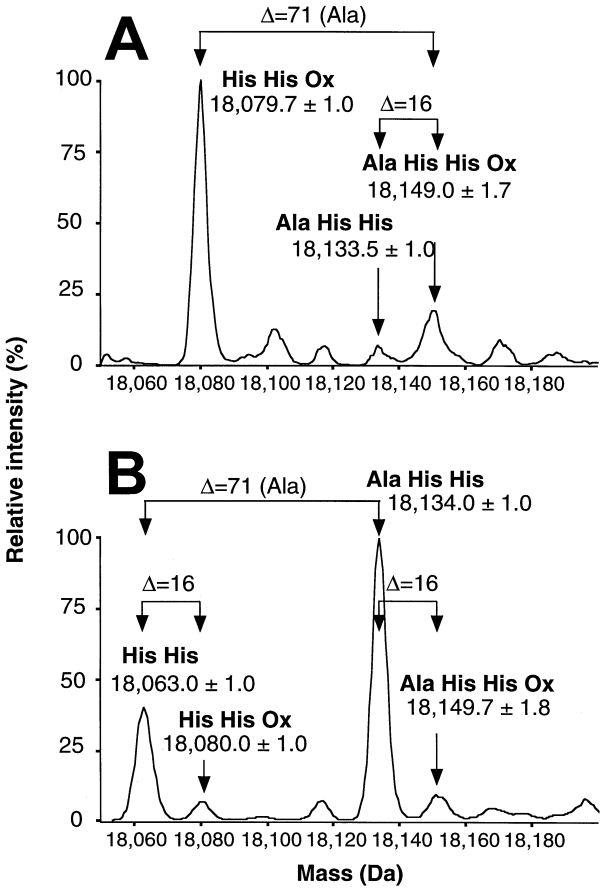

Fig. 2. Comparison of mass spectra of native and recombinant OBP. (A) Reconstructed ion spray mass spectrum and N-terminal sequence of natural OBP-1F isolated from the rinsed olfactory epithelium. (B) Reconstructed ion spray mass spectrum of recombinant OBP-1F secreted by *P. pastoris* with its native signal peptide. His–His Ox and His–His are the oxidized and normal forms of OBP-1F with His–His at their N terminus, respectively. Ala–His–His–Ox and Ala–His–His are the corresponding forms with an extra Ala at their N-terminal end. Δ indicates the mass difference between peaks shown by arrows.

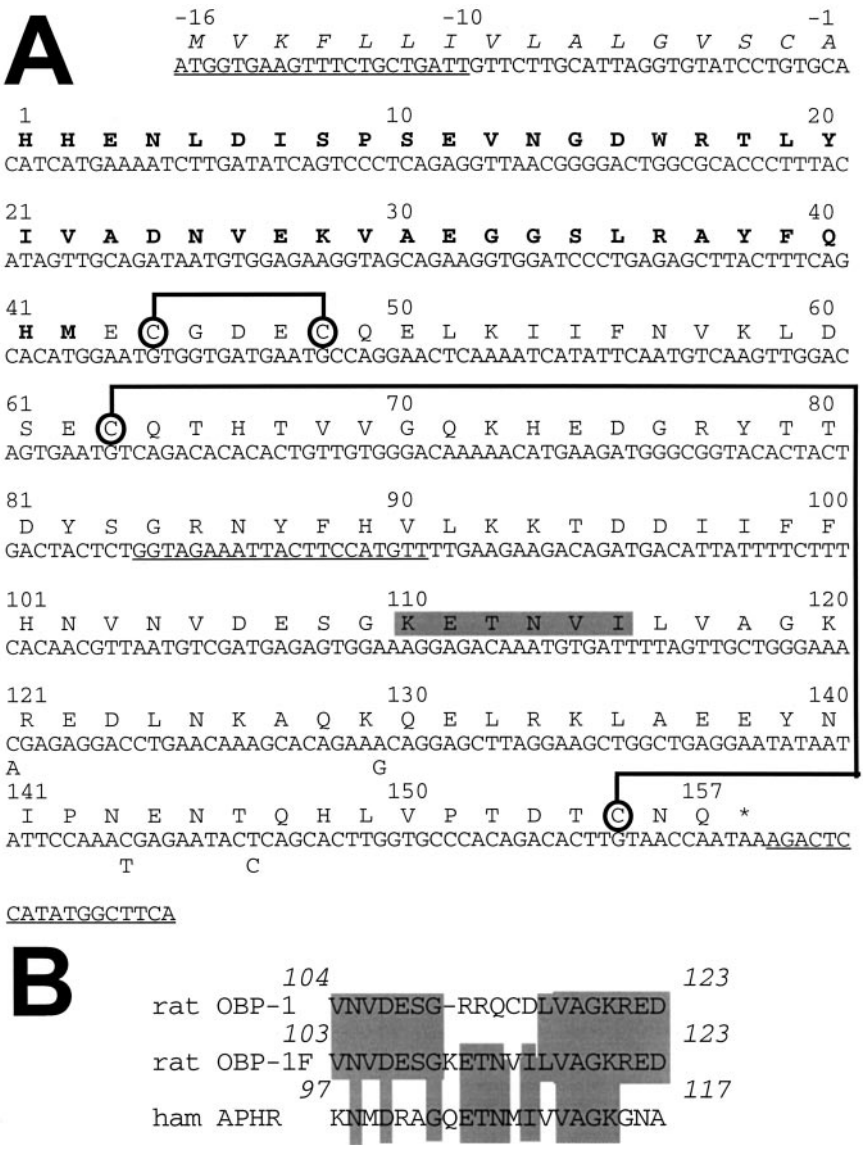

Fig. 3. cDNA cloning and sequence of OBP-1F. (A) Nucleotide sequence of a cDNA clone corresponding to OBP-1F and the deduced amino acid sequence. Amino acids are numbered from the first His of the mature sequence. Amino acids identified by N-terminal sequencing are in bold and the signal peptide is in italics. The two nucleotide sequences used to design primers are underlined. The asterisk marks the stop codon. Base variations (silent mutations) are indicated below the main nucleotide sequence at amino acid positions 121, 129, 143 and 146. The disulfide bond pairings are indicated by lines connecting the half-cystines. The amino acids sequence that differs from the OBP-1 sequence [12] is shaded gray. (B) Local comparison in this area of the amino acid sequences of OBP-1F with those of OBP-1 [12] and aphrodisin [32]. Conserved amino acids are shaded gray.

Volatile-odorant binding assay

Bovine α-lactalbumin was obtained from Sigma. Purified OBP-1F and α-lactalbumin were dissolved in 50 μL of 500 mM potassium phosphate buffer pH 7.5 to a final concentration of 1.65 mM. Twelve 500-μL glass tubes, containing control buffer, OBP-1F and α-lactalbumin solutions, were incubated overnight at 25 °C in a 2-L sealed glass chamber containing a pure undiluted odorant (10 μL in the chamber) which evaporated freely. The proteins and the control buffer were then extracted

Table 1. Identification of proteins isolated from the olfactory epithelium mucus. Molecular masses and N-terminal or internal amino acid sequences of proteins identified in the mucus rinsed from the olfactory epithelium.

Molar mass[a]	Sequence	Identification	Swissprot access number
4963	SDKPDMAEIE[b]	Thymosine B-4	TYB4_Mouse (P20065)
8582	MQIFVKTLTG[b]	Ubiquitine T-54	UBIQ_HUMAN (P02248)
15 746	XXAVXVLKGD[b]	Superoxide dismutase	SODC_Rat (P07632)
15 837	AVXXXKG	Superoxide dismutase	SODC_Rat (P07632)
76 751	VPDKTVKWXA	Siderophilin	TRFE_RAT (P12346)
18 502	NVVLDKPGKV	Olfactory marker protein	OMP_RAT (P08523)
18 793		Olfactory marker protein	OMP_RAT (P08523)
65 333	EAHKSEIAHR[b]	Serum albumin	ALBU_RAT (P02770)
15 198	VLSADDKTNI[b]	Hemoglobin α chain	HBA_RAT (01946)
42 648	PFSNSHNTQK[b]	Creatine kinase B chain	KCRB_RAT (P07335)
18 177	HHENLDISPS[b]	Odorant-binding protein	OBP-1F (AJ251322)[c]

[a] Masses measured by MALDI-TOF MS. [b] N-terminal sequence. [c]EMBL accession number.

at room temperature with 50 μL chloroform and analyzed by GC using a GC 8000 Series 8180 Fisons Instruments (Thermoquest) equipped with an on-column injector and FID detector (300 °C). The analytical column used was a DB-1 column (30 m × 0.32 mm, i.d. 0.25 μm; J & W Scientific, Interchim, France) with a deactivated precolumn. The oven temperature gradient was applied from 60 °C to 200 °C at 10 °C·min^{-1} and then raised to 290 °C at 20 °C·min^{-1}. The carrier gas was helium at 8.7 mL·min^{-1}. Odorants diluted in chloroform were used for calibration.

RESULTS

Characterization of mucus proteins

After dissection, the olfactory epithelium was rinsed with buffer and submitted to ion-exchange HPLC. Table 1 describes the identification of the chromatographic peaks obtained through MALDI-TOF and microsequencing analysis after reversed-phase HPLC purification of each fraction and for some peaks after N-deblocking by trifluoracetic acid treatment [31]. Numerous proteins were identified among which were creatine kinase, hemoglobin α chain, serum albumin, siderophilin, superoxide dismutase, thymosine, ubiquitin, an olfactory marker protein and a protein whose N-terminus was homologous to OBP-1 [12]. Figure 1 shows the reversed-phase chromatogram of the OBP-containing fraction. Only one peak was identified as a rat OBP, exhibiting the same N-terminal sequence as OBP-1 up to the 42nd residue, except it began at position 2 of the known sequence [12]. Nevertheless, a minor contaminating sequence was found with the exact N-terminus of OBP-1. No other OBP-like sequence was observed. A LC–MS experiment was conducted on the ion-exchange chromatography fraction containing the OBP-like sequence to analyze precisely the size of the natural molecule. Figure 2A shows the reconstructed mass spectrum, which was composed of several isoforms. The major one had a mass of 18 079.7 ± 1 Da, whereas two minor forms were observed with masses of 18 133.5 ± 1 Da and 18 149.0 ± 1.7 Da. The latter molecule was more abundant and differed by one oxygen atom, suggesting oxidation of a methionine residue. None of these molecules had the same size as the previously described OBP-1 (calculated mass of 18 037.9 Da with formed disulfide bonds and without the N-terminal Ala).

Cloning and sequencing of a novel rat OBP variant

Two oligonucleotide probes were designed according to the rat OBP-1 clone published by Pevsner *et al.* [12] in order to amplify the coding cDNA sequence from a cDNA library originating from the total rat olfactory epithelium mRNA (Fig. 3A). Six clones were obtained exhibiting point mutations restricted at nucleotide positions 409, 435, 477 and 486. They were all silent mutations encoding the same amino acids. A clone of 540 nucleotides encoding a protein of 173 residues including a signal peptide of 16 amino acids is shown in Fig. 3A. The amino acid sequence is numbered starting at His, the first of the 42 residues of the major form of the mature protein determined by microsequencing. It was found to be very close to that of OBP-1 with a variation occurring at a single region (positions 110–115) but quite different from another rat olfactory protein, OBP-2, described by Dear *et al.* [19,20]. We therefore named this novel protein variant OBP-1F (F for Fisher rat strain). The comparison between OBP-1 and OBP-1F is emphasized in Fig. 3B. In the region 110–115, OBP-1F exhibited an insertion and no amino acid homology with OBP-1 was observed. Nevertheless, a strong homology was found with the hamster aphrodisin in this region [32,33], while no other known OBP was found to share this internal sequence.

OBP-1F heterologous expression and purification

In order to evaluate its binding properties, OBP-1F was expressed using the methylotrophic yeast *P. pastoris*. The protein was secreted using either the yeast prepropeptide signal from the *Saccharomyces cerevisiae* α mating factor peptide (pAlfOBP) with Glu–Ala–Glu–Ala as spacer or its native rat signal peptide (pNatOBP). Approximately 500 His$^+$ transformants of the GS115 strain were obtained by electroporation and 24 transformants corresponding to Mut^s phenotypes were screened for each contruction. The higher producing clones were screened by SDS/PAGE to determine the amount of OBP-1F secreted into the extracellular medium. The comparison of the highest producing clones showed that the construct using the yeast α mating factor prepropeptide signal was five times more efficient than the construct using the native rat signal peptide. Samples of the expression medium supernatants, taken at various time intervals, were also analyzed

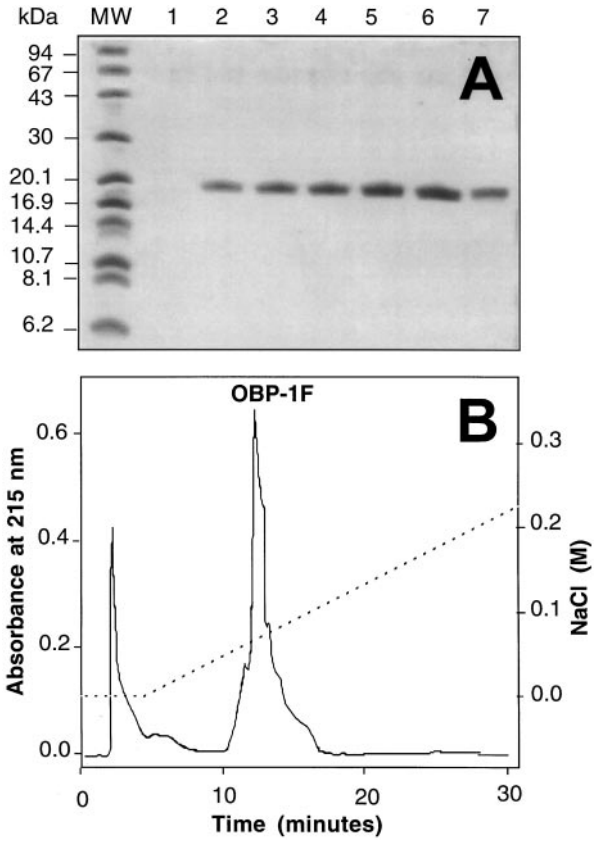

Fig. 4. Expression and purification of the recombinant OBP-1F. (A) Kinetics of recombinant OBP-1F secretion by *P. pastoris* using the α factor signal peptide, followed by SDS/PAGE. The lane marked MW shows molecular mass standards (Pharmacia PMW kit) and lanes 1–6 are 10-μL aliquots of a 0–5-day culture supernatant. Lane 7 shows purified recombinant OBP-1F. (B) Recombinant OBP-1F purification by ion-exchange chromatography on a Vydac QAE column (300 VHP, 0.75 i.d. × 5 cm). OBP-1F was eluted with a NaCl gradient in 20 mM Tris/HCl pH 8.0 (dashed line) from 0 to 0.5 M for 50 min.

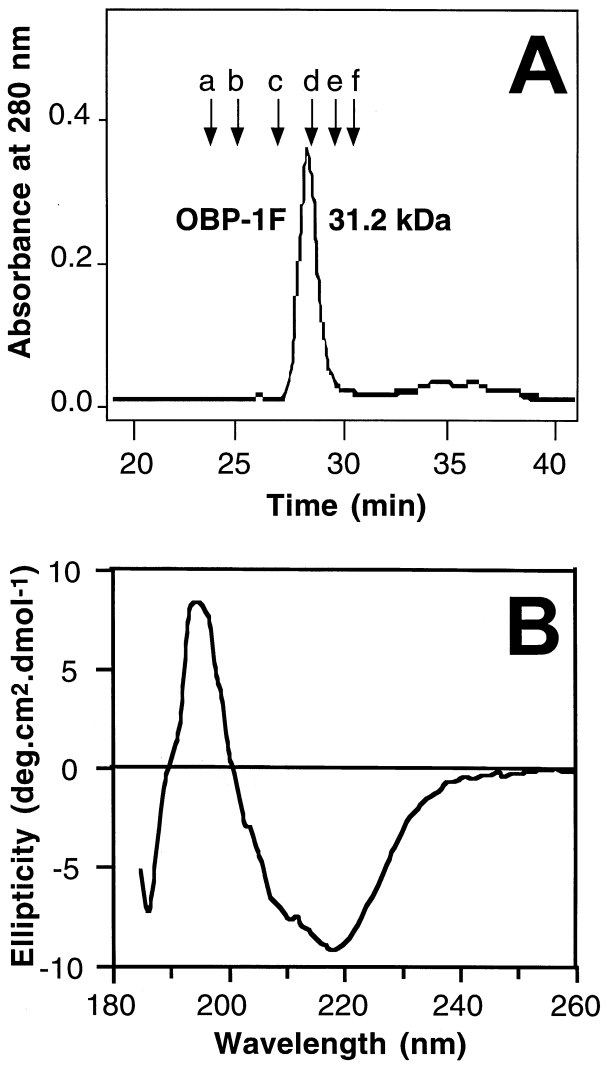

Fig. 5. Secondary and quaternary structure of the recombinant OBP-1F. (A) Exclusion-diffusion chromatography on Superose 12. The elution positions of the molecular mass standards are indicated by arrows: a, BSA (67 kDa); b, chicken egg ovalbumin (43 kDa); c, dimeric bovine β-lactoglobulin (36 kDa); d, carbonic anhydrase (30 kDa); e, soybean trypsin inhibitor (21.5 kDa); f, bovine ribonuclease A (13.7 kDa). (B) Secondary structure determination by CD spectroscopy. Protein concentration was approximately 1 mg·mL^{-1} and path length 0.01 cm.

by PAGE to determine the optimal induction time. Only a single band of recombinant protein, migrating at 18 kDa, was detectable by Serva blue G staining. Figure 4A shows the protein expression kinetics of the construct with the yeast α-mating factor prepropeptide signal. The electrophoretic profile reveals that the protein regularly accumulated for 5 days without proteolytic degradation of the recombinant protein, as confirmed by MS (data not shown), while no other protein was detectable. Approximately 80 mg·L^{-1} of purified protein were obtained over an expression period of 5 days.

After centrifugation, the yeast culture filtrate was submitted to ion-exchange HPLC. Figure 4B shows that the recombinant protein eluted at 95 mM NaCl like the native mucus protein (data not shown). A last purification step was conducted through gel filtration in order to remove any possible small ligand. SDS/PAGE analysis of the purified protein is shown in Fig. 4A (lane 7).

Recombinant protein characterization

N-terminal sequencing and LC–MS were performed to analyze the recombinant OBP-1F expressed with the natural rat signal peptide (Fig. 2B). Several molecules were observed that could be gathered into two groups, the most abundant (≈ 80%, based on sequencing) with Ala–His–His as the N-terminus, and the other with His–His (≈ 20%). In the first group, a major protein

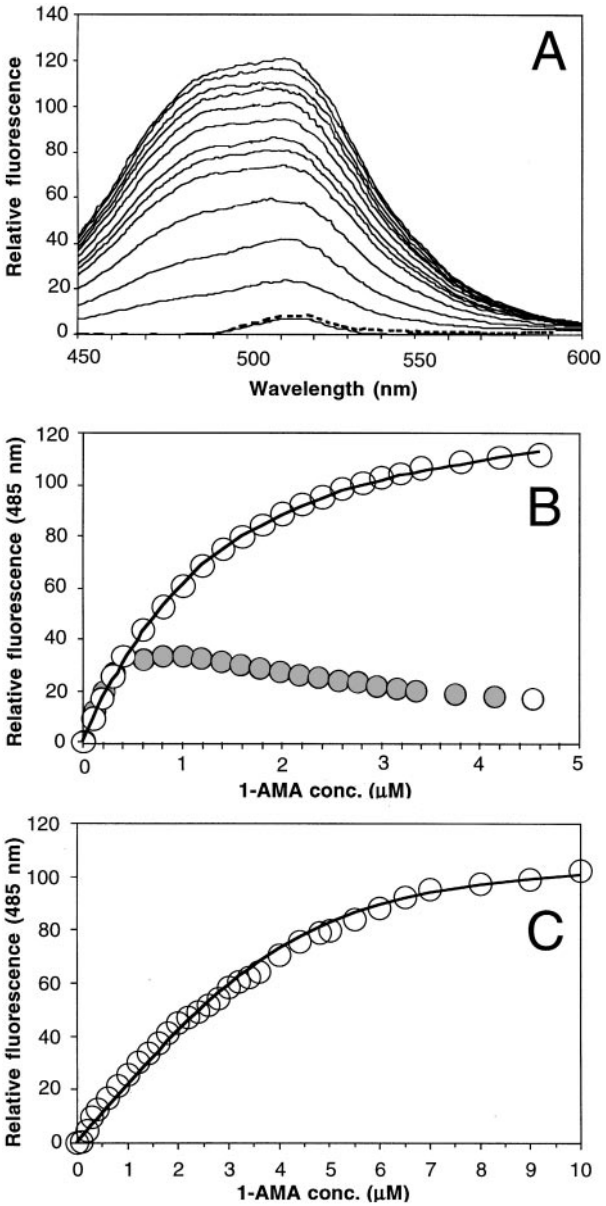

Fig. 6. 1-AMA fluorescence binding assay. (A) Fluorescence emission spectra of 1-AMA in presence of recombinant OBP-1F. Spectra recorded at 25 °C correspond to 1-AMA concentrations from 0.1 to 4.6 μM. Dashed line indicates the fluorescence of 1-AMA alone (2 μM). (B) Binding curves: ○, titration with 1-AMA added as 1 μL successive aliquots of a solution in 10% MeOH; ●, additions as solution in 95% EtOH. Excitation wavelength was 255 nm, emission wavelength 485 nm, protein concentration 4 μM. (C) 1-AMA binding curve on OBP-1F at 10 μM in the same conditions.

was found to have a molecular mass of 18 134.0 ± 1.0 Da. This is in perfect agreement with the mass of the natural protein (18 133.5 ± 1.0 Da) and with that deduced from the cDNA sequence (18 135.0 Da) with Ala–His–His at the N terminus and two disulfide bridges ascertained by the sulfhydryl group titration (< 0.25 thiol per molecule was found). An additional minor peak exhibited a molecular mass of 18 149.7 ± 1.8 Da with a mass excess of 15.7 ± 2.0 Da attributed to methionine oxidation. This minor peak was also observed in the natural protein (Fig. 2A). In the second group, the molecular mass of the major peak was found to be 18 063.0 ± 1.0 Da in agreement with that deduced from the cDNA sequence with His–His at the N terminus and two formed disulfide bridges (18 064.0 Da). As in the other group, an additional minor peak exhibited a mass excess of 17 ± 2.0 Da probably due to oxidation. This minor peak exhibited exactly the same mass as the major form observed in the natural protein (Fig. 2A). When the construction with the α factor prepropeptide was used the molecular masses and sequences of the recombinant proteins were observed in accordance with those expected. Nevertheless the additional spacer sequence was not properly cleaved, leaving three forms in equivalent amount beginning with Glu–Ala–Glu–Ala–Ala–His, Glu–Ala–Ala–His and Ala–His.

To determine the disulfide bridge pairing, unreduced OBP-1F was hydrolyzed with Glu-C endoproteinase and the digest submitted to LC–MS analysis. A peptide peak eluted at 9.6 min with an average molecular mass of 2834.9 ± 0.4 Da. It corresponded to the sum of the masses of the two peptides N145–Q157 (C terminus) and C63–E74 linked by a disulfide bond (calculated molecular mass of 2835.1 Da). In addition, the PVDF band corresponding to the collection of this peak was submitted to Edman sequencing. Two sequences were determined in equimolar amounts (≈ 1 pmol) for 10 cycles. They confirmed that these two peptides were associated by a disulfide bond between C63 and C155. The peptide composed of two chains joined by the remaining cysteines could not be observed in the conditions used. Nevertheless the second disulfide bridge was assigned to occur between C44 and C48 (Fig. 3A) as no free sulfhydryl group was detected by the Ellman reagent.

Calibrated exclusion-diffusion chromatography of purified OBP-1F at 1.0 mg·mL^{-1} gave an apparent molecular mass of 31.2 kDa, which is approximately twice the value obtained from MS, demonstrating dimerization of the recombinant protein at neutral pH (Fig. 5A). Figure 5B shows the CD spectrum of the recombinant OBP-1F in phosphate buffer. The shape of the spectrum, i.e. the maximum at 195 nm and the minimum at 217 nm, clearly showed the presence of a high percentage of β-sheet in the protein. The deconvolution of the measured spectrum revealed an average 61% of β sheet and very little or no α helix.

Fluorescence binding assay with 1-AMA

As described by Paolini *et al.* [34,35] for porcine OBP-1, 1-AMA proved also to be a ligand for the rat OBP-1F. When excited at 255 nm, 1-AMA presented a weak fluorescence emission with a maximum at 515 nm probably due to some light scattering effect (Fig. 6A, dashed line). In the presence of the protein, the

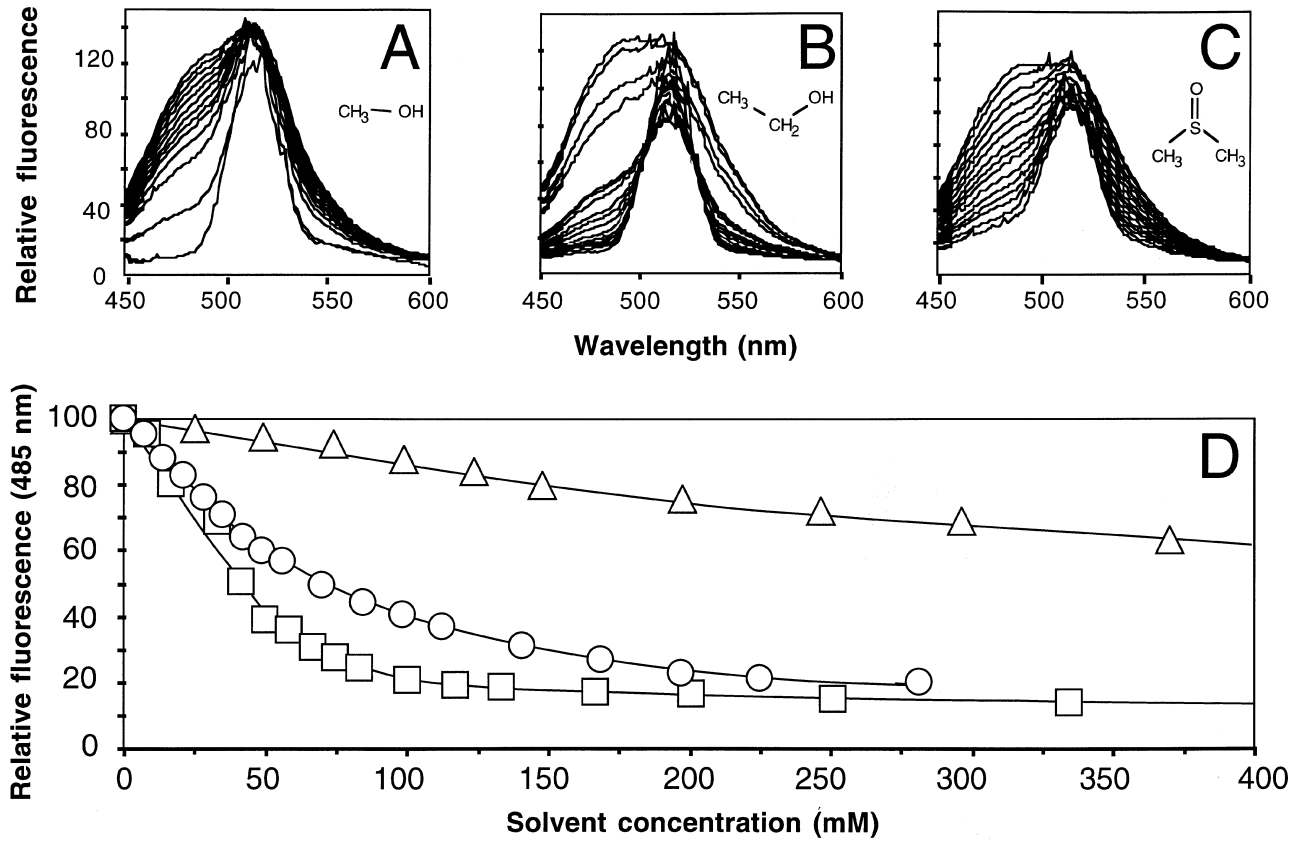

Fig. 7. 1-AMA fluorescence quenching upon solvent binding. Competitive binding assays between 1-AMA and MeOH (A), EtOH (B) and dimethylsulfoxide (C). Spectra were recorded at 25 °C with an excitation wavelength of 255 nm. OBP-1F and 1-AMA concentrations were 2 μM. (A) MeOH concentrations from 24.7 to 990 mM; (B) EtOH concentrations from 8.4 to 500 mM; (C) Dimethylsulfoxide concentrations from 7 to 282 mM (D) Binding curves of OBP-1F with 1-AMA followed by fluorescence at 485 nm (excitation wavelength 255 nm): MEOH (△), ETOH (□) and dimethylsulfoxide (○).

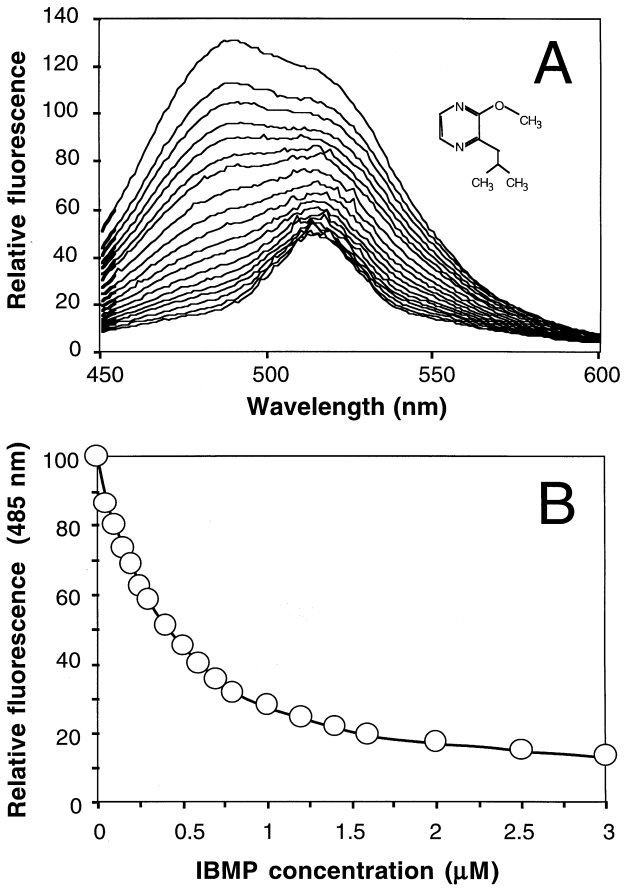

Fig. 8. 1-AMA fluorescence quenching upon 2-isobutyl-3-methoxypyrazine binding. (A) Competitive binding assays between 1-AMA and IBMP. IBMP concentrations varied from 0.05 to 3 μM. Spectra were recorded at 25 °C with an excitation wavelength of 255 nm. OBP-1F and 1-AMA concentrations were 2 μM (B) Binding curve of 1-AMA fluorescence at 485 nm bound to OBP-1F quenched by IBMP (○).

emission spectrum showed another maximum at 485 nm corresponding to specific 1-AMA fluorescence (Fig. 6A). We noted only a 15-fold quantum yield increase at 485 nm instead of 80 as observed with the porcine OBP-1 [35]. Figure 6A shows the binding of 1-AMA as followed by fluorescence, the intensity of which is saturable. Assuming that the protein was saturable by 1-AMA, as strongly suggested by titration curves, we used the fluorescence intensity at 485 nm to calculate the relative amount of bound 1-AMA. Figure 6B shows that the fluorescence titration curve was greatly modified when EtOH was used as solvent for 1-AMA. Consequently we used 10% MeOH to determine the binding parameters with a 10-μM OBP-1F solution to ensure its dimeric state (not shown). Figure 6C shows the saturation curve, which was adjusted by nonlinear regression according to the procedure of Norris and Li [30]. An apparent affinity constant of 0.6 ± 0.3 μM was found. The number of binding sites was observed to be 0.4 ± 0.3 per monomer, which would suggest that one dimeric OBP-1F molecule binds one 1-AMA molecule.

MeOH, EtOH and dimethylsulfoxide were then tested for their ability to quench the fluorescence of 1-AMA bound to OBP-1F (Fig. 7A–C). We observed that the 485 nm emission maximum was much more changed than the maximum at 515 nm, probably due to light scattering. We therefore followed the displacement of 1-AMA at 485 nm. EtOH was indeed shown to be a competitive ligand when added to OBP-1F complexed with 1-AMA (Fig. 7B), whereas dimethylsulfoxide and MeOH were also observed to be competitors (Fig. 7A and C). Figure 7D illustrates the displacement of 1-AMA by solvents and shows that EtOH caused the chase of half of the 1-AMA molecules at 45 mM, a value close to that obtained with dimethylsulfoxide (50 mM), while MeOH was a far less efficient competitor. Consequently, we carefully avoided dissolving 1-AMA in EtOH and preferably used 10% MeOH for further experiments. The fluorescence binding assay has been used in experiments aimed to test a classical odorant (2-isobutyl-3-methoxypyrazine) (Fig. 8A). We observed that IBMP was able to displace 1-AMA quite efficiently (Fig. 8B). It was able to chase half of the 1-AMA molecules from OBP-1F at 0.3 μM, which is far less than EtOH (45 mM) and dimethylsulfoxide (50 mM).

VOBA

The large quantity of *P. pastoris* secreted OBP-1F permitted the setting up of a novel assay to mimic the *in vivo* uptake of airborne molecules by OBP in conditions close to those of the perireceptor physiology. Purified OBP-1F and a control protein (bovine α-lactalbumin, a protein that does not bind hydrophobic molecules such as odorants) were dissolved in neutral phosphate buffer to a high concentration (1.65 mM) comparable to the concentration of OBP in mucus [36]. Protein solutions were placed in a sealed glass chamber containing a pure odorant not diluted in any solvent, with buffer as control. The proteins and the control buffer were then extracted with chloroform and analyzed by GC. The bovine α-lactalbumin solution did not solubilize any tested odorant more efficiently than the buffer alone (data not shown). Figure 9A shows the comparison of the binding onto OBP-1F of seven odorants of different chemical structures and odors (IBMP, linalool, isoamyl acetate, 1-octanal, 1-octanol, dimethyl disulfide and

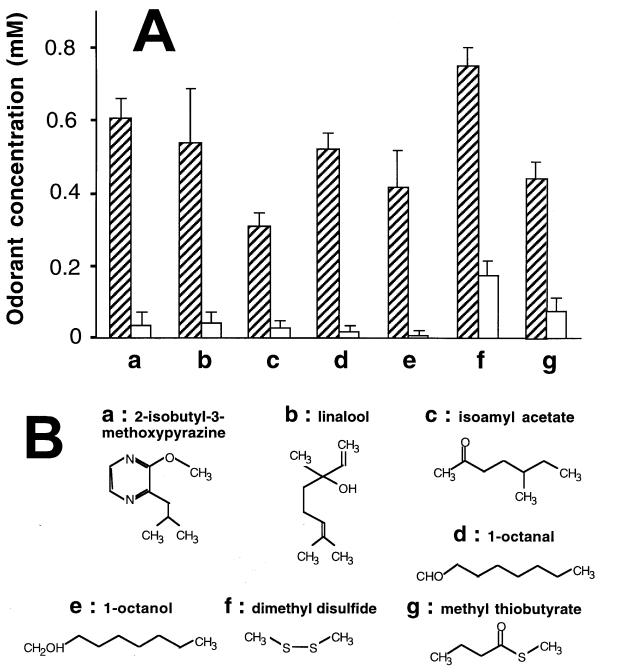

Fig. 9. VOBA. (A) Binding of airborne odorants onto OBP-1F (1.65 mM) in 500 mM phosphate buffer, pH 7.5 (hatched bars) and onto the buffer alone (open bars) determined by GC (a, IBMP; b, linalool; c, isoamyl acetate; d, 1-octanal; e, 1-octanol; f, dimethyl disulfide; g, methyl thiobutyrate), bars indicate standard deviations. (B) Chemical structure of the odorants tested.

methyl thiobutyrate), whose structure is presented in Fig. 9B. All of these odorants bound very strongly to OBP-1F, while their amount in the aqueous buffer remained very low (with the exception of dimethyl disulfide which is known to be slightly soluble in water). With the exception of isoamyl acetate, most of the odorants were found bound to OBP-1F at a concentration very close to half that of the protein. IBMP was previously observed to totally chase 1-AMA at 1 μM. In VOBA, its concentration was at least 20 μM in buffer, which strongly suggests that OBP-1F is saturated. As shown in Fig. 9, the amount of odorant bound per OBP-1F molecule was found to be 0.4–0.45. The comparison of the affinity of the various molecules for OBP-1F is not relevant as odorants were applied in large excess.

DISCUSSION

Only one OBP, close to the previously described rat OBP-1 [12] was found among the olfactory epithelium proteins, which were solubilized from the nasal mucus collected on the epithelium and dissected free from the vomeronasal organ by rinsing with buffer different from that used by other groups. Contamination by OBP-2, a putative vomeronasal organ protein [19,20], was not observed because it should have been excluded from the chromatographic analysis due to its basic isoelectric point. The novel OBP variant, named OBP-1F, exhibited four isoforms that vary in their N-terminal sequences and their degree of oxidation. The major natural OBP-1F begins with His–His and presents an oxidized methionine, while two minor forms have Ala–His–His at their N-terminus, one of them presenting an oxidized Met. The perfect agreement between the measured molecular mass and that calculated from the cDNA sequence shows that no glycosylation occurs in natural OBP-1F, contrary to aphrodisin [32].

The *P. pastoris* expression system was chosen for rat OBP-1F because it allows the production of large quantities of soluble disulfide-bonded proteins [23,37]. When using the natural signal peptide, the recombinant OBP-1F produced was comparable in primary structure to the natural protein, and exhibited the same isoforms with some variation in their relative abundance. All of the isoforms had their disulfide bonds formed whereas the natural molecule was more oxidized than the recombinant ones. In addition, CD proved that the recombinant molecules were in the correct conformational state. Although much more efficient from a quantitative point of view, the use of the α factor signal peptide with the spacer sequence Glu–Ala–Glu–Ala led to a random N-terminus, different from that of the natural protein, as already reported for another lipocalin, β-lactoglobulin [38]. The yeast secretion machinery is therefore able to properly process secretory proteins with a mammal peptide signal without proteolytic degradation in our culture conditions. The protein produced was easy to purify in absence of any sequence alteration such as the addition of a His tag, as *P. pastoris* secretes only very low levels of its own proteins into the medium.

In addition to the amputation of the N-terminal residue, the cDNA deduced amino acid sequence of OBP-1F presents a local clear difference from that of OBP-1 [12] between positions 110 and 116 and a close similarity for this portion with that of the hamster aphrodisin [32,33]. The origin of this difference could arise in the genotype difference of the rat strain used, which was not mentioned by Pevsner *et al*. [12], but is presumed to be a Sprague–Dawley strain. It is striking to note that we identified six cDNA clones with silent mutations in the cDNA library. These variants could arise from either multiple genes or RNA editing.

CD showed that recombinant OBP-1F was indeed folded in to a secondary structure expected for a lipocalin [39–41]. MS coupled with sequencing allowed the assignment of the two disulfide bridges (C44–C48, C63–C155) for the first time in a rat OBP. In spite of a gap in the sequence numbering, aphrodisin exhibits the same disulfide bonds, but at positions 38–42 and 57–149 [32]. The comparison with the porcine OBP-1 shows that, in absence of other cysteines, only the second disulfide bond is conserved [9,34]. In the mouse major urinary protein, this bridge (found at positions 68–161) was also observed, whereas Cys142 remained unbonded [42]. This disulfide bond, which immobilizes the C-terminal structure formed by an α helix and an antiparallel β-strand, appears therefore to be more important for the global structure of the molecule than the other one. When we investigated the quaternary structure of OBP-1F, we found it exists as a dimer at neutral pH such as that described for the recombinant OBP-1 [22] and the bovine OBP, which is devoid of cysteine [7,8]. The porcine OBP-1 is, nevertheless, known to exist as a monomer [5,9]. No correlation can therefore be inferred between OBP oligomerization and their disulfide bonding.

As regards the number of odorant binding sites, both the fluorescence experiments and the amount of odorants bound to OBP-1F observed with VOBA in saturating conditions (typically for IBMP) suggest the occurrence of a single binding site per dimer. Such a stoichiometry was observed with the bovine OBP [11,43], but proved different from porcine OBP-1, which has been shown to bind 1-AMA with an equimolar monomer stoichiometry [35]. The occurrence of inactive forms is unlikely because no heterogeneity was observed by any of the numerous very precise approaches we used to characterize the molecule (MS, Edman sequencing, reversed-phase LC) in a proportion sufficient to explain a number of sites lower than one per monomer. It is then tempting to postulate that the rat OBP-1F binding site is located at the interface of the two monomers as it has been suggested by Tegoni *et al*. [8] in the case of the bovine OBP. The dissociation constant found for 1-AMA (0.6 ± 0.3 μM) is close to that of the porcine OBP-1 (1.3 μM) [35]. Only the emission at 485 nm was significantly affected when solvents (EtOH, dimethylsulfoxide and MeOH) or an odorant molecule (IBMP) were used to displace 1-AMA, whereas the other maximum remained unaltered. The maximum at 515 nm was due to light scattering, caused by the absence of cut-off filter in our experiments. When compared with porcine OBP-1, the environment of the fluorophore binding site should nevertheless be more hydrophilic for OBP-1F, since the quantum yield of 1-AMA bound to this protein is five times weaker [35]. In addition, whereas porcine OBP-1 induces 1-AMA fluorescence at 481 nm, we noted a fluorescence maximum at a larger wavelength (485 nm).

The displacement of 1-AMA by various organic volatile solvents usually used in odorant-binding experiments led us to hint technical cautions about the use of these solvents in olfaction studies. These observations might explain the discrepancy of the OBP affinity constants for odorants found by different teams [36]. For instance Löbel *et al*. [22] found a K_d of 1.7 μM for IBMP uptake by rat OBP-1, while others reported 20 μM. In addition, the ability of EtOH to efficiently bind OBP-1F raises the question of how it can disturb the aroma perception in alcoholic beverages.

The understanding of the uptake of the volatile odorants by the OBP in the nasal mucus needs the development of an assay

as close as possible as the natural conditions. The large amounts of produced OBP-1F permitted us to set up a biomimetic assay of general use to identify and compare the binding of numerous unlabeled odorants onto OBP in almost physiological conditions. VOBA has the great advantage of avoiding the use of solvents that can cause interference with OBP binding, because they can themselves be ligands for OBP; neither does it depend on the use of radioactively labeled molecules. In combination with MS coupled with GC, VOBA can be adapted to odorant screening and to binding competition tests. It can also be used in the investigation of airborne compound binding onto olfactory receptors; it has permitted observations on the binding by OBP-1F of volatile odorants of different chemical structures and odors, strengthening the role of OBPs as specific volatile hydrophobic odorant carriers, as neither the control protein nor the aqueous buffer bound significant amounts of these odorants. In addition, heterologous expression of OBP opens the possibility for site-directed mutagenesis of specific residues in order to investigate and clearly define the relationships between the structure and the function of these proteins.

ACKNOWLEDGEMENTS

We thank D. Trotier (CNRS, Massy, France) for skillful aid in rat dissection and helpful discussion. This work was supported by the French Institut National de la Recherche Agronomique and by the Association pour la Recherche sur le Cancer.

REFERENCES

1. Steinbrecht, R.A. (1998) Odorant-binding proteins: expression and function. *Ann. N.Y. Acad. Sci.* **855**, 323–332.
2. Pelosi, P. (1996) Perireceptor events in olfaction. *J. Neurobiol.* **30**, 3–19.
3. Bignetti, E., Cavaggioni, A., Pelosi, P., Persaud, K.C., Sorbi, R.T. & Tirindelli, R. (1985) Purification and characterization of an odorant-binding protein from cow nasal tissue. *Eur. J. Biochem.* **149**, 227–231.
4. Garibotti, M., Navarrini, A., Pisanelli, A.M. & Pelosi, P. (1997) Three odorant-binding proteins from rabbit nasal mucosa. *Chem. Senses* **22**, 383–390.
5. Dal Monte, M., Andreini, I., Revoltella, R. & Pelosi, P. (1991) Purification and characterization of two odorant-binding proteins from nasal tissue of rabbit and pig. *Comp. Biochem. Physiol.* **99**, 445–451.
6. Pes, D. & Pelosi, P. (1995) Odorant-binding proteins of the mouse. *Comp. Biochem. Physiol.* **112**, 471–479.
7. Bianchet, M.A., Bains, G., Pelosi, P., Pevsner, J., Snyder, S.H., Monaco, H.L. & Amzel, L.M. (1996) The three-dimensional structure of bovine odorant binding protein and its mechanism of odor recognition. *Nature Struct. Biol.* **3**, 934–939.
8. Tegoni, M., Ramoni, R., Bignetti, E., Spinelli, S. & Cambillau, C. (1996) Domain swapping creates a third putative combining site in bovine odorant binding protein dimer. *Nature Struct. Biol.* **3**, 863–867.
9. Spinelli, S., Ramoni, R., Grolli, S., Bonicel, J., Cambillau, C. & Tegoni, M. (1998) The structure of the monomeric porcine odorant binding protein sheds light on the domain swapping mechanism. *Biochemistry* **37**, 7913–7918.
10. Pes, D., Dal Monte, M., Ganni, M. & Pelosi, P. (1992) Isolation of two odorant-binding proteins from mouse nasal tissue. *Comp. Biochem. Physiol.* **103**, 1011–1017.
11. Pevsner, J., Trifiletti, R., Strittmatter, S.M. & Snyder, S.H. (1985) Isolation and characterization of an olfactory receptor protein for odorant pyrazine. *Proc. Natl Acad. Sci. USA* **82**, 3050–3054.
12. Pevsner, J., Reed, R.R., Feinstein, P.G. & Snyder, S.H. (1988) Molecular cloning of odorant-binding protein: member of a ligand carrier family. *Science* **241**, 336–339.
13. Pelosi, P., Baldaccini, E. & Pisanelli, A.M. (1982) Identification of a specific olfactory receptor for 2-isobutyl-3-methoxypyrazine. *Biochem. J.* **201**, 245–248.
14. Felicioli, A., Ganni, M., Garibotti, M. & Pelosi, P. (1993) Multiple types and forms of odorant-binding proteins in the old-world porcupine. *Comp. Biochem. Physiol.* **105**, 775–784.
15. Miyawaki, A., Matsushita, F., Ryo, Y. & Mikoshiba, K. (1994) Possible pheromone-carrier function of two lipocalins in the vomeronasal organ. *EMBO J.* **13**, 5835–5842.
16. Pes, D., Mameli, M., Andreini, I., Krieger, J., Weber, M., Breer, H. & Pelosi, P. (1998) Cloning and expression of odorant-binding proteins Ia and Ib from mouse nasal tissue. *Gene* **212**, 49–55.
17. Utsumi, M., Ohno, K., Kawasaki, Y., Tamura, M., Kubo, T. & Tohyama, M. (1999) Expression of major urinary protein genes in the nasal glands associated with general olfaction. *J. Neurobiol.* **39**, 227–236.
18. Ganni, M., Garibotti, M., Scaloni, A., Pucci, P. & Pelosi, P. (1997) Microheterogeneity of odorant-binding proteins in the porcupine revealed by N-terminal sequencing and mass spectrometry. *Comp. Biochem. Physiol.* **117B**, 287–291.
19. Dear, T.N., Boehm, T., Keverne, E.B. & Rabbitts, T.H. (1991) Novel genes for potential ligand-binding proteins in subregions of the olfactory mucosa. *EMBO J.* **105**, 775–784.
20. Dear, T.N., Campbell, K. & Rabbitts, T.H. (1991) Molecular cloning of putative odorant-binding and odorant-metabolizing proteins. *Biochemistry* **30**, 10376–10382.
21. Ohno, K., Kawasaki, Y., Kubo, T. & Tohyama, M. (1996) Differential expression of odorant-binding protein genes in the rat nasal glands: implication of odorant-binding protein II as a possible pheromone transporter. *Neuroscience* **71**, 355–366.
22. Löbel, D., Marchese, S., Krieger, J., Pelosi, P. & Breer, H. (1998) Subtypes of odorant-binding proteins. Heterologous expression and ligand binding. *Eur. J. Biochem.* **254**, 318–324.
23. Briand, L., Perez, V., Huet, J.-C., Danty, E., Masson, C. & Pernollet, J.-C. (1999) Optimization of the production of a honeybee odorant-binding protein by *Pichia pastoris*. *Prot. Exp. Purif.* **15**, 362–369.
24. Schägger, H. & von Jagow, G. (1987) Tricine-sodium dodecyl sulfate-polyacrylamide gel electrophoresis for the separation of proteins in the range from 1 kDa to 100 kDa. *Anal. Biochem.* **166**, 368–379.
25. Sallantin, M., Huet, J.-C., Demarteau, C. & Pernollet, J.-C. (1990) Reassessment of commercially available molecular weight standards for peptide sodium dodecyl sulfate-polyacrylamide gel electrophoresis using electroblotting and microsequencing. *Electrophoresis* **11**, 34–36.
26. Nespoulous, C., Huet, J.-C. & Pernollet, J.-C. (1992) Structure–function relationships of α and β elicitins, signal proteins involved in the plant–*Phytophthora* interaction. *Planta* **186**, 551–557.
27. Pace, C.N., Vajdos, F., Fee, L., Grimsley, G. & Gray, T. (1995) How to measure and predict the molecular absorption coefficient of a protein. *Protein Sci.* **4**, 2411–2423.
28. Deléage, G. & Geourjon, C. (1993) Interactive and graphic coupling between multiple alignments, secondary structures prediction and motif/pattern scanning into protein sequences. *Comput. Applic. Biosci.* **9**, 87–91.
29. Ellman, G.L. (1958) A colorimetric method for determining low concentrations of mercaptans. *Arch. Biochem. Biophys.* **74**, 443–450.
30. Norris, A.W. & Li, E. (1998) Fluorometric titration of the CRABPs. In *Retinoid Protocols. Methods in Molecular Biology*, Vol. 89 (Redfern, C.P.F., ed.), pp. 123–139. Humana Press Inc, Totowa, NJ, USA.
31. Gheorghe, M.T., Jörnvall, H. & Bergman, T. (1997) Optimized alcoholytic deacetylation of N-acetyl-blocked polypeptides for subsequent Edman degradation. *Anal. Biochem.* **254**, 119–125.
32. Henzel, W.J., Rodriguez, H., Singer, A.G., Stults, J.T., Macrides, F., Agosta, W.C. & Niall, H. (1988) The primary structure of aphrodisin. *J. Biol. Chem.* **263**, 16682–16687.

33. Mägert, H.J., Cieslak, A., Alkan, O., Luscher, B., Kauffels, W., Forssmann, W.G., Singer, A.G., Agosta, W.C., Clancy, A.N. & Macrides, F. (1999) The golden hamster aphrodisin gene. Structure, expression in parotid glands of female animals, and comparison with a similar murine gene. *J. Biol. Chem.* **274**, 444–450.
34. Paolini, S., Marchese, S., Scaloni, A. & Pelosi, P. (1998) Amino acid sequence, post-translational modifications, binding and labelling of porcine odorant-binding protein. *Chem. Senses* **23**, 689–698.
35. Paolini, S., Tanfani, F., Fini, C., Bertoli, E. & Pelosi, P. (1999) Porcine odorant-binding protein: structural stability and ligand affinities measured by Fourier-transform infrared spectroscopy and fluorescence spectroscopy. *Biochim. Biophys. Acta* **1431**, 179–188.
36. Pelosi, P. (1994) Odorant-binding proteins. *Crit. Rev. Biochem. Mol. Biol.* **29**, 199–228.
37. Danty, E., Briand, L., Michard-Vanhée, C., Perez, V., Arnold, G., Gaudemer, O., Huet, D., Huet, J.-C., Ouali, C., Masson. C. & Pernollet, J.-C. (1999) Cloning and expression of a queen-pheromone binding protein in the honeybee, an olfactory-specific, developmentally regulated protein. *J. Neurosci.* **19**, 7468–7475.
38. Denton, H., Smith, M., Husi, H., Uhrin, D., Barlow, P., Batt, C. & Sawyer, L. (1998) Isotopically labeled bovine β-lactoglobulin for NMR studies expressed in *Pichia pastoris*. *Prot. Exp. Purif.* **14**, 97–103.
39. Flower, D.R., North, A.C.T. & Attwood, T.K. (1993) Structure and sequence relationships in the lipocalins and related proteins. *Protein Sci.* **2**, 753–761.
40. Flower, D.R. (1995) Multiple molecular recognition properties of the lipocalin protein family. *J. Mol. Recog.* **8**, 185–195.
41. Flower, D.R. (1996) The lipocalin protein family: structure and function. *Biochem. J.* **318**, 1–14.
42. Böcskei, Z., Groom, C.R., Flower, D.R., Wright, C.E., Phillips, S.E.V., Cavaggioni, A., Findlay, J.B.C. & North, A.C.T. (1992) Pheromone binding to two rodent urinary proteins revealed by X-ray crystallography. *Nature* **360**, 186–188.
43. Pevsner, J., Hou, V., Snowman, A.M. & Snyder, S.H. (1990) Odorant-binding protein, characterization of ligand binding. *J. Biol. Chem.* **265**, 6118–6125.